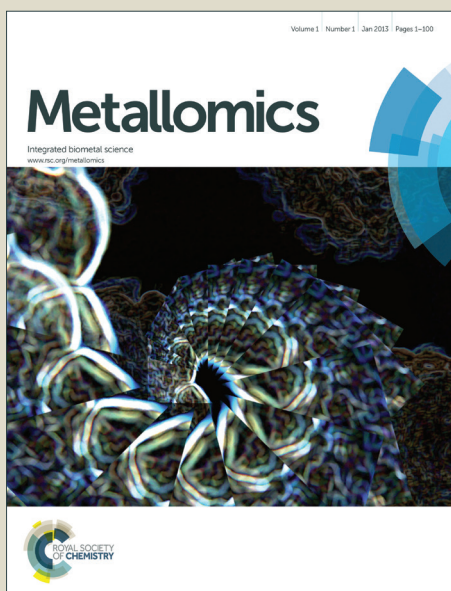


Metallomics

Accepted Manuscript



This is an *Accepted Manuscript*, which has been through the Royal Society of Chemistry peer review process and has been accepted for publication.

Accepted Manuscripts are published online shortly after acceptance, before technical editing, formatting and proof reading. Using this free service, authors can make their results available to the community, in citable form, before we publish the edited article. We will replace this *Accepted Manuscript* with the edited and formatted *Advance Article* as soon as it is available.

You can find more information about *Accepted Manuscripts* in the [Information for Authors](#).

Please note that technical editing may introduce minor changes to the text and/or graphics, which may alter content. The journal's standard [Terms & Conditions](#) and the [Ethical guidelines](#) still apply. In no event shall the Royal Society of Chemistry be held responsible for any errors or omissions in this *Accepted Manuscript* or any consequences arising from the use of any information it contains.

DMT1 iron uptake in the PNS: bridging the gap between injury and regeneration

Rocio Martinez Vivot¹, Guillermo Copello², Celeste Leal³, Gonzalo Piñero¹, Vanina Usach¹, Mijael Rozenszajn¹, Laura Morelli⁴, Clara Patricia Setton-Avruj¹.

¹ Departamento de Química Biológica, Facultad de Farmacia y Bíoquímica, Universidad de Buenos Aires. Instituto de Química y Físicoquímica Biológica (IQUIFIB), UBA-CONICET, Buenos Aires, Argentina.

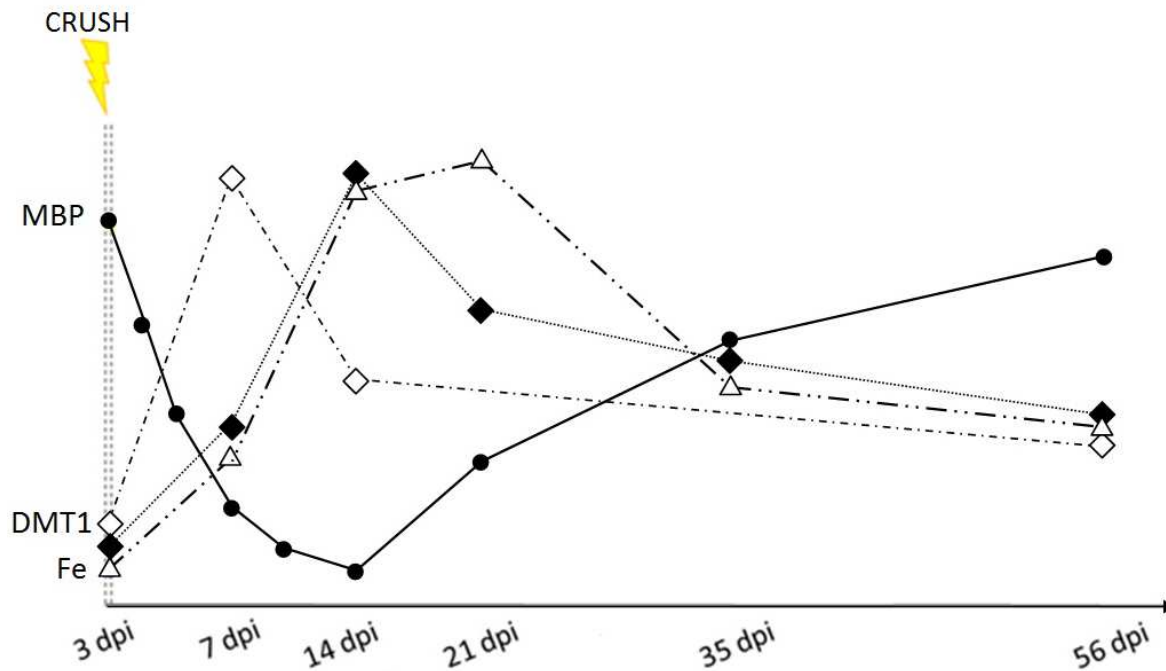
² Cátedra de Química Analítica Instrumental, Facultad de Farmacia y Bioquímica, Universidad de Buenos Aires, Buenos Aires, Argentina.

³ Laboratorio de Terapias Regenerativas y Protectoras del Sistema Nervioso Central, Fundación Instituto Leloir. IIBBA-CONICET, Buenos Aires, Argentina

⁴ Laboratorio de Amiloidosis y Neurodegeneración. Fundación Instituto Leloir. IIBBA- CONICET, Buenos Aires, Argentina.

This manuscript was elaborated with the invaluable contribution of late Dr Luis Díaz, Cátedra de Química Analítica Instrumental, Facultad de Farmacia y Bioquímica, Universidad de Buenos Aires, Buenos Aires, Argentina.

Table of contents:



This work supports DMT1 involvement in iron regulation in SC, its role as a sensor of iron necessity and its ability to guarantee iron supply during myelination and remyelination

1
2
3
4
5
6
7
8
9
10
11
12
13
14
15
16
17
18
19
20
21
22
23
24
25
26
27
28
29
30
31
32
33
34
35
36
37
38
39
40
41
42
43
44
45
46
47
48
49
50
51
52
53
54
55
56
57
58
59
60

Abstract

Previous work by our group demonstrated the key role of iron in Schwann cell maturation through an increase in cAMP, PKA activation and CREB phosphorylation. These studies opened the door to further research on a non-transferrin-bound iron uptake, which revealed the presence of DMT1 mRNA all along SC progeny, hinting at a constitutive role of DMT1 in ensuring the provision of iron in the PNS. In light of these previous results, the present work evaluates the participation of DMT1 in the remyelination process following a demyelinating lesion promoted by sciatic nerve crush –a reversible model of Wallerian degeneration. DMT1 was observed to colocalize with SC marker S100 β at all survival times analyzed. In turn, the assessment of DMT1 mRNA expression exhibited an increase 7 days post-injury, while DMT1 protein levels showed an increase 14 days after crush at the lesion site and distal stump; finally, an increase in iron levels became evident as from 14 days post-injury, in parallel with DMT1 values. To sum up, the present work unveils the role of DMT1 in mediating the neuroregenerative action of iron.

Key words: DMT1, iron, Schwann cell, Wallerian degeneration

Abbreviations: Schwann cells (SC), Myelin basic protein (MBP), Myelin protein zero (P₀), Cyclic adenosine monophosphate (cAMP), Protein kinase A (PKA), Cyclic adenosine monophosphate (cAMP), cAMP responding binding element (CREB), Divalent metal transporter type 1 (DMT1), Peripheral Nervous System (PNS), transferrin (Tf), transferrin receptor (TfR), iron responsive elements (IRE), Wallerian degeneration (WD), non-transferrin bound iron (NTBI)

Introduction

Iron deficiency is a high-incidence disorder which affects approximately 2,000 million people worldwide (1) and which may lead to irreversible damage in the nervous system when occurring during the first two years of life. This is a consequence of the key role iron plays in metabolic functions in multiple nervous system processes, in particular, myelinogenesis.

The classical perspective of intracellular iron metabolism involved the participation of three proteins: transferrin (Tf), which is capable of transporting two Fe^{3+} atoms, Tf receptor (TfR), essential for iron uptake, and ferritin, the main iron storage protein. Later findings on myelinogenesis demonstrated that iron uptake in the brain exceeded Tf capacity as a carrier, which gave way to the notion of a Tf-independent transport system (2). This notion was further explored and the participation of divalent metal transporter 1 (DMT1) in the central nervous system (CNS) is now generally accepted (3, 4; 5).

As for the peripheral nervous system (PNS), the importance of iron lies in its capacity to promote the differentiation of Schwann cells (SC), the population responsible for peripheral myelin biosynthesis. On the basis of findings showing the essential role of cAMP in myelin gene expression in SC, our group demonstrated an iron-promoted increase in oxidative species followed by an increase in cAMP levels, PKA activation and CREB phosphorylation (6, 7) in cultured SC and their consequent maturation into a myelinating phenotype. Furthermore, we have recently shown the presence of DMT1 in SC plasma membrane *in vivo* and *in vitro*, which suggests its participation in cellular iron uptake (8).

DMT1 is a four-isoform protein –including two iron-responsive-element-positive (IRE+) and two IRE- isoforms– ubiquitously expressed at systemic and cellular levels. It is generally regarded as one of the major transport proteins for iron uptake and considered sensitive to a wide range of normal and abnormal circumstances regarding damage and adaptive mechanisms involved in recovery (9). DMT1 has three well characterized functions associated to three different locations: a) it delivers iron to the cytosol on the endosomal membrane (10, 11,12), b) it mediates Fe^{2+} uptake by the intestinal lumen on

1
2
3 the enterocyte brush border membrane (13, 14), c) it is responsible for non-Tf-bound iron
4 (NTBI) uptake on the plasma membrane (15, 16, 8). These three functions are critical for
5 iron homeostasis at cellular level and highlight the relevance of DMT1 participation both
6 through the classical TfR-mediated pathway –at endosomal level– and the NTBI pathway.
7 On the whole, however, bibliographical evidence hints at a weak correlation between Tf-
8 bound iron uptake and neurodegenerative processes, while NTBI uptake has proven to be
9 closely connected (17).

10
11 In this context, the present work evaluates the role of DMT1 in the regulation of
12 iron levels along demyelination-remyelination post-sciatic nerve crush, a reversible model
13 of Wallerian degeneration (WD) characterized by inflammation and myelin breakdown, as
14 a result of the interruption of axon-SC cross-talk. To this end, DMT1 mRNA and protein
15 expression were assessed, together with iron content, at different survival times after
16 nerve crush.
17
18
19
20
21
22
23
24
25
26
27
28
29

30 **Results**

31 *Persistence of DMT1 expression in SC all along the demyelination-remyelination process*

32
33 Immunohistochemical studies were conducted in order to determine whether
34 DMT1 colocalization with SC is preserved after sciatic nerve crush. The positive
35 immunoreaction of DMT1 coincided with that of S100 β , a well-known SC marker, at all
36 survival times evaluated, that is 7, 14, 21, 35 and 56 days post-injury. In all cases,
37 Manders' coefficient was over 0.6, which confirms the persistence of DMT1 expression in
38 SC all along the demyelination-remyelination process. Two survival times were selected as
39 examples: one of incipient demyelination (7 days post-injury) and another of complete
40 remyelination (56 days post-injury) (Fig. 1 and 2, respectively). The remaining days were
41 also analyzed and rendered equivalent results (data not shown).
42
43
44
45
46
47
48
49
50
51

52 *Increase in DMT1 protein levels after sciatic nerve crush*

53
54 DMT1 quantification in the contralateral nerve and the different areas of the
55 ipsilateral nerve was determined through Western blot studies and expressed as a
56
57
58
59
60

1
2
3 percentage of control nerve levels. The contralateral nerve and the proximal area of the
4
5 ipsilateral nerve showed no significant differences with the control nerve at any of the
6
7 time points studied. In contrast, and as from 7 days post-injury, the crush and distal areas
8
9 evidenced an increase in DMT1 levels, which peaked at 14 days and persisted until 56 days
10
11 post-injury (Fig. 3 and Table 1).

12
13 As no significant differences were observed in DMT1 levels between control and
14
15 sham nerves at any of the survival times studied (data not shown), results were analyzed
16
17 in reference to control nerves.

18 19 20 *Increase in DMT1 mRNA after sciatic nerve crush*

21
22 To assess whether the increments observed in protein levels were mediated by
23
24 increments in transcript levels, DMT1/TBP mRNA expression was evaluated at the time
25
26 points considered of greatest interest, including a point previous to protein peak time (7
27
28 days post-injury), peak time (14 days post-injury) and as long as two months after the
29
30 crush, when remyelination was already complete and DMT1 protein levels were still high.
31
32 In the same way, the areas chosen for RT-qPCR analysis were those where the percentage
33
34 of increment had rendered significant variations, i.e. the crush and distal area of the
35
36 ipsilateral nerve. When considering two variables such as survival time and area, a sham
37
38 nerve of each survival time was included in the analysis as an internal control. As results
39
40 showed no significant differences between these sham nerves and control ones at any of
41
42 the survival times analyzed (data not shown), DMT1 mRNA levels were expressed as a
43
44 fold-change regarding the control nerve.

45
46 In both the crush and distal areas, results showed a 2-fold increase in DMT1 mRNA
47
48 expression 7 days post-injury and a 0.5-fold increase at 14 days. At 56 days post-injury,
49
50 although still significantly elevated in the crush and distal areas, mRNA levels presented a
51
52 downward tendency in the crush area (Fig. 4 and Table 1).

Higher iron levels after sciatic nerve crush

After demonstrating the increase in DMT1 mRNA expression and protein levels in the crush and distal areas, iron levels as a measure of transporter activity were evaluated in the ipsilateral and contralateral nerves at 7, 14, 21, 35 and 56 days post-injury.

Again, as results showed no significant differences in iron content between control and sham nerves at any of the survival times analyzed (data not shown), iron quantification in the contralateral nerve and the different areas of the ipsilateral nerve was determined through atomic absorption spectroscopy and expressed as a percentage of control nerve levels.

No significant differences were detected at 7 days post-injury regardless of area; in contrast, as from 14 days post-injury, the crush and distal stumps exhibited an increase in iron levels (Fig. 5 and Table 1). When considering iron content evolution over time in each of the areas, no significant differences were found in the contralateral nerve and proximal stump as compared to a control nerve. In contrast, a peak between 14 and 21 days post-injury was observed in the crush and distal areas, in line with results observed in DMT1 protein levels (Fig. 5 and 6).

Discussion

The PNS exhibits a remarkable regeneration ability rooted in SC phenotype plasticity, which entails a cross-talk between SC and axons. The interruption of this cross-talk as a consequence of neuron-free SC culture and the demyelination process associated to axotomy or crush both promote SC dedifferentiation into an immature-like SC phenotype, evidenced by a decrease in MBP levels. The reestablishment of this cross-talk allows SC to recover a mature phenotype, as reflected by myelin protein levels (18, 19). Bibliographical references connecting PNS regeneration and iron metabolism are scarce and date back to the 1990s. These references, derived from experiments conducted mostly in axolotls, report that their amputated limbs were regenerated only in the presence of iron salts (20) and that Tf content in neurons and SC evidenced a 20-fold increase during the regeneration process (21). In mammals, work by Ravich et al. (22)

1
2
3 proved a 60-80% increase in TfR levels, specific Tf binding and iron uptake after rat sciatic
4
5 nerve crush.
6

7 In contrast, the effects of iron have long been proven necessary for successful
8 development in the CNS (23, 24) and an accumulating body of evidence highlights its
9 importance in central myelinogenesis (25, 26, 27, 28, 29, 30, 31). Moreover, its deficiency
10 has long-lasting effects even after being compensated (32, 33). In the light of these
11 findings, the role of iron in peripheral myelinogenesis becomes a challenging field of
12 research.
13
14
15
16
17

18 Previous work on PNS iron uptake focused on TfR actions. Although TfR levels are
19 known to be basally low in control nerves, previous work by our group reported an
20 increase at 7 and 14 days post-injury (34), in agreement with results by Raivich et al. (21)
21 showing a strong and transient increase in TfR levels upon nerve injury and regeneration.
22 In contrast, DMT1 mRNA is expressed all along SC progeny (8), regardless of the presence
23 of injury. This crucial difference has led us to infer a constitutive role for DMT1 ensuring
24 the provision of iron, whose prodifferentiating effects (7) make it an essential factor in
25 PNS myelinogenesis. These results spearhead the study of DMT1 in the PNS and provide
26 support for its participation in ensuring iron uptake along the degeneration-regeneration
27 process.
28
29
30
31
32
33
34
35
36

37 Immunohistochemical studies revealed the colocalization of DMT1 with S100 β ,
38 which demonstrates the presence of DMT1 in SC even during a demyelinating process.
39 The increase in DMT1 protein levels and iron content hints at a positive correlation
40 between transporter expression and activity during WD; in contrast, a negative
41 correlation, depicted by a specular image, may be thought to exist between DMT1 and
42 MBP levels in the crush and distal stump of the demyelinated nerve (Fig. 6). Its mRNA
43 expression dynamics unveils DMT1 functionality by generating an increase in protein
44 levels at moments of maximum iron necessity and the subsequent increase in its content.
45 In addition, the persistently high levels of DMT1 and its spatial and temporal pattern
46 support our hypothesis.
47
48
49
50
51
52
53
54
55
56
57
58
59
60

1
2
3
4
5
6
7
8
9
10
11
12
13
14
15
16
17
18
19
20
21
22
23
24
25
26
27
28
29
30
31
32
33
34
35
36
37
38
39
40
41
42
43
44
45
46
47
48
49
50
51
52
53
54
55
56
57
58
59
60

Once again, while PNS data appear to be scarce, iron accumulation has been widely associated with inflammatory processes in CNS neurodegenerative disorders such as Parkinson's and Alzheimer's disease (35). In addition, pro-inflammatory interleukins have been shown to promote iron accumulation through an increase in DMT1 mRNA and a decrease in ferroportin mRNA, which has proven to have a deleterious effect (36). In contrast to CNS data, our findings prove that the increase in DMT1 levels and the promotion of iron accumulation have a beneficial impact on the remyelination process in the PNS. These *in vivo* results also find support in our *in vitro* studies reporting the role of iron in cultured SC maturation (7) and are in line with previous findings on the connection between iron deficiency and immune response suppression (37, 38). Furthermore, recent findings on lung metal-related injury and oxidative stress support DMT1 involvement in the regulation of pulmonary inflammation, probably by operating at the level of macrophage phagolysosomes (37, 39).

As for some neurodegenerative diseases, the increase in DMT1 levels might not be a direct consequence of the increase in intracellular iron after injury but a secondary consequence of the inflammatory processes involved in WD (40, 41). Several factors appear to contribute to the pro-inflammatory environment created 7 days post-injury, including a peak in IL-6 and TGF- β 1 secretion and the recruitment of macrophages. Seven days post-injury also seems to be a crucial time point in iron metabolism, as evidenced by the peak in DMT1 mRNA expression and the increasing tendency observed in DMT1 protein levels as from 7 days post-injury, which might trigger an increase in intracellular iron. This increase may be partly responsible for inducing macrophage transition from a pro-inflammatory to an anti-inflammatory response (42) and thus create, together with the increase in IL-10, an anti-inflammatory environment. These findings, combined with our results showing the highest iron levels 14-21 days post-injury when the inflammatory response is fading out, all hint to a cross-talk involving DMT1, iron status and inflammation. On the whole, this transitory peak in DMT1 appears to ensure an increase in iron content to foster PNS remyelination.

Experimental designs

Materials

Sucrose, leupeptin, pepstatin A, Coomassie blue, bovine serum albumin, penicillin, streptomycin, Hoechst 32258 were purchased from Sigma Chem. Co (St. Louis, MO, USA). TRIZOL reagent, Oligreen, SuperScript II reverse transcriptase and KAPA SYBER FAST qPCR Master Mix kit were purchased from Invitrogen (Grand Island, NY, USA), oligo-dT was purchased from Integrated DNA Technologies (Coralville, IA, USA), M-MLV reverse transcriptase and Taq DNA polymerase were purchased from Promega. Fetal calf serum (FCS) was purchased from Natocor (Córdoba, Argentina). PVDF membranes and ECL Plus kit were provided by GE Healthcare (Little Chalfont, UK). NRAMP2 (DMT1) and S100 β antibody was purchased from Santa Cruz Biotechnology Inc. (Santa Cruz, CA, USA). Secondary antibodies for immunocytochemistry, immunohistochemistry, and Western blot studies were purchased from Jackson (West Grove, PA, USA). The fluorescent mounting media was from Dako North America Inc. (Carpinteria, CA, USA). Cryoplast was purchased from Biopack (Buenos Aires, Argentina).

For atomic absorption studies, nitric acid (HNO₃) was from J.T. Baker (Phillipsburg, NJ, EE.UU.), chloroform (HCCl₃) was provided by Sintorgan (Buenos Aires, Argentina), magnesium nitrate (Mg (NO₃)₂) and the standard iron solution were purchased from Carlo Erba (Rodano, Italy).

Animals

Adult Wistar rats (70-day old) were anesthetized with ketamine (75 mg/kg i.p.) and xylazine (10 mg/kg i.p.), and their right sciatic nerves were exposed and crushed for 8 seconds at mid-thigh level and thus denominated ipsilateral nerve and analytically divided into three areas namely proximal, crush and distal, as previously described (43). The animals were allowed to survive for 7, 14, 21, 28, 35 and 56 days, after which experiments were performed. Contralateral nerves were used as internal controls, in addition to sham (surgically treated non-crushed) and naïve (untreated) nerves.

1
2
3 All procedures were performed in accordance with the guidelines of the
4 Committee of Bioethics of Facultad de Farmacia y Bioquímica, Universidad de Buenos
5 Aires.
6
7
8
9

10 *Preparation of samples for Western blot analysis*

11
12 Sciatic nerves from adult rats were homogenized in lysis buffer [20 mM Hepes (pH
13 7.9), 350 mM NaCl, 20% glycerol, 1% NP-40, 1 mM MgCl₂, 0.5 mM EDTA and 0.1 mM EGTA,
14 1 mM DTT, 0.1% PMSF, and leupeptin 10 mg/mL], sonicated and centrifuged at 15,000
15 rpm at 4°C for 15 min. The supernatant was stored at -80°C and protein concentration was
16 determined by the Bradford method.
17
18
19
20

21
22 Proteins (40 µg/lane) were separated by SDS-PAGE on 12.5% gels and
23 electroblotted onto PVDF membranes. Non-specific protein binding sites were blocked for
24 2 h at room temperature with blocking buffer containing 5% non-fat dry milk in PBS-
25 Tween 20 0.1%. Rabbit anti-DMT1 (1:500) was used as primary antibody and peroxidase-
26 conjugated anti-rabbit IgG (1:10,000) as secondary antibody. Immunoreactivity was
27 visualized with the ECL Plus kit using a Storm 840 Phosphorimager (Molecular Dynamics,
28 Sunnyvale, CA, USA) and analyzed using Image Quant 4.1 software.
29
30
31
32
33
34

35
36 Total protein in each lane was quantified using Fast Green, as β-actin, β-tubulin
37 and GAPDH are not reliable in WD processes (44,45).
38
39
40

41 *Preparation of tissue sections for immunohistochemistry*

42
43 Adult Wistar rats were deeply anesthetized (ketamine 75 mg/kg i.p and xylazine 10
44 mg/kg i.p.) and perfused through the heart with 200 mL warm (37°C) PBS followed by 100
45 mL of fixative (4% paraformaldehyde in 1 x PBS, pH 7.4) at 4°C. The sciatic nerves were
46 removed and post-fixed in the same solution overnight at 4°C. The tissue was rinsed in
47 15% sucrose in PBS at 4°C for at least 24 h and then rinsed in 30% sucrose in PBS and
48 stored at -80°C until processed.
49
50
51
52
53

54
55 Tissues were cut into 16-µm sections with a cryostat (Leica) and the sections were
56 mounted onto gel-precoated glass slides and stored at -20°C. The slides were rinsed twice
57
58
59
60

1
2
3 in PBS and twice in PBS-Triton X-100 0.1%. After blockade in 5% FCS overnight at 4°C,
4
5 slides were incubated for 18-24 h in a humid chamber at 4°C with mouse anti-S100β (SC
6
7 marker) (1:100) and rabbit anti-DMT1 (1:200) antibodies, diluted in PBS containing 1%
8
9 FCS. Samples were rinsed three times in PBS and incubated at room temperature for 2 h
10
11 with Cy3 (1:200) or Cy2 (1:200)-labeled secondary antibodies plus Hoechst 32258 (2μg/mL
12
13 in PBS) and later rinsed three times in PBS for another 5 min each time. Sections were
14
15 coverslipped with Dako Fluorescent Mounting Medium. Controls were done by incubation
16
17 without the primary antibodies. Images were acquired using either an Olympus BX50
18
19 epifluorescence microscope provided with a Cool-snap digital camera or an Olympus
20
21 FV1000 confocal microscope.

22 To study the colocalization of different cell markers, the overlap coefficient
23
24 according to Manders (R) was estimated using Image Pro Plus software (version 5.1) and
25
26 values over 0.6 were considered positive colocalization (46).

27 28 29 *RNA Isolation and RT-qPCR*

30
31 Total RNA was extracted from sciatic nerves using TRIZOL reagent and purified
32
33 according to the manufacturer's instructions. RNA content was assessed by absorbance at
34
35 260 nm and its purity was determined by the ratio A260/A280. The quality of total
36
37 isolated RNA was controlled by electrophoresis on 1% agarose gel. Total RNA extracted
38
39 from whole nerves was used for cDNA synthesis by reverse transcription as described
40
41 below.

42
43 One μg total RNA was reverse transcribed using the oligo-dT primer plus DMT1 R:
44
45 5'- ACA GGA GAT TGA TGG CGA TG -3' and SuperScript II reverse transcriptase. cDNA was
46
47 amplified by SYBR Green RT-qPCR with an Mx3005P cycler (Stratagene, La Jolla, CA, USA).
48
49 Cycling conditions were as follows: 94 °C for 10 min, 94 °C for 30 s, annealing for 1 min at
50
51 58 °C, and 72 °C for 30 s for 40 cycles. The DMT1 primers used were F: 5'- CTT GCA CCT
52
53 TGC TGA AGT G -3' and R: 5'- ACA GGA GAT TGA TGG CGA TG -3'. Melt curve analysis and
54
55 agarose gels verified the formation of a single desired PCR product. The relative amount of
56
57 transcripts to TATA-binding protein (F: 5'-ACC GTG AAT CTT GGC TGT AA-3' and R: 5'- CCG
58
59
60

1
2
3 TGG CTC TCT TAT TCT CA-3') was quantified by the 2- $\Delta\Delta$ Ct method using MxPro software.
4
5 The relative expression of the genes in sciatic nerve homogenates was determined by
6
7 comparison of Ct using the following equation: 2- $\Delta\Delta$ Ct, considering $\Delta\Delta$ Ct= Δ Ct_{sample} -
8
9 Δ Ct_{control} [Δ Ct_{sample}=(Ct_{DMT1} - Ct_{TBP})_{sample} and Δ Ct_{control}=(Ct_{DMT1} - Ct_{TBP})
10
11 control](47, 48).
12
13

14 15 *Iron quantification by atomic absorption spectroscopy*

16
17 Lysis buffer was pre-treated with chitosan hydrogel in constant agitation at room
18
19 temperature overnight in order to remove iron contamination from the reagents. Equal
20
21 volumes of HNO₃ 10% and sample (100 μ l) were left for digestion overnight at 37°C (49).
22
23 Samples were then centrifuged and, after the addition of HCl₃ (50 μ l) and
24
25 recentrifugation, the aqueous phase was recovered. Extracts were diluted 1:50 with 0.05%
26
27 HNO₃. Both samples and standards were measured by triplicate using Mg(NO₃)₂ (1000
28
29 ppm) as a matrix modifier in an atomic absorption spectrometer with a graphite furnace
30
31 Buck Scientific VGP 210 (E. Norwalk, CT, USA). Electrothermal atomization was carried out
32
33 using a pyrolytic graphite tube, and absorbance was collected at 248.3 nm, with 0.2 nm
34
35 slit, ash temperature of 1400°C and atomization 2800°C.
36

37 38 *Statistical analyses*

39
40 Statistical analyses were performed between experimental groups by applying
41
42 two-way ANOVA, using Infostat software. Error estimation for the two-way ANOVA was
43
44 performed with SPSS software checking that sphericity, variance homogeneity (Levene
45
46 test) and normality (Shapiro-Wilks) applied to the samples analyzed. Situations that
47
48 turned out to be significantly different were compared by DGC (Di Rienzo, Guzmán y
49
50 Casanoves, 2002) and Tukey's test. Significance was set at p <0.05.

51
52 We also verified that the groups used as reference (control, sham and
53
54 contralateral) did not differ statistically.
55
56
57
58
59
60

Conclusion

The evidence presented here sheds light on a vastly unexplored field, i.e. PNS iron metabolism, and supports the notion of DMT1 involvement in iron regulation in SC (50, 51, 52), its role as a sensor of iron necessity and its ability to guarantee iron supply during myelination and remyelination. The mechanisms underlying these roles may include DMT1 parallel dynamics with TfR levels, Tf mRNA expression and iron requirements (33). Taken together, our findings reinforce the potential properties of DMT1 as a therapeutic target against neurodegeneration (17) and pave the way for promising future research.

1
2
3
4
5
6
7
8
9
10
11
12
13
14
15
16
17
18
19
20
21
22
23
24
25
26
27
28
29
30
31
32
33
34
35
36
37
38
39
40
41
42
43
44
45
46
47
48
49
50
51
52
53
54
55
56
57
58
59
60

Acknowledgements:

The authors thank Dr María Victoria Rosato-Siri and Ms María Marta Rancez for their assistance in the elaboration of this manuscript.

This study was supported by grants from the University of Buenos Aires (UBACYT 20020100101017) and CONICET (PIP 830 and PIP 567).

Authors declare no conflict of interest.

References

1. J Beard. *Report of a Joint World Health Organization/Centers for Disease Control and Prevention Technical Consultation on the Assessment of Iron Status at the Population Level*, World Health Organization/Centers for Disease Control, Geneva, 2004.
2. T Moos, EH Morgan, *J. Neurosci. Res.*, 1998, **54**, 486-494.
3. H Lee, X Zhu, G Liu, S Chen, G Perry, MA Smith, H Lee, *Cell Research*, 2010, **20**, 397-399
4. J Salazar, N Mena, S Hunot, A Prigent, D Alvarez-Fischer, M Arredondo, C Duyckaerts, V Sazdovitch, L Zhao, LM Garrick, MT Nuñez, MD Garrick, R Raisman-Vozari, EC Hirsch, *Proc. Natl. Acad. Sci. USA*, 2008, **105(47)**, 18578-8
5. Y Ke, ZM Qian, *Progress in Neurobiology*, 2007, **83**, 149-173
6. C Salis, CJ Goedelmann, JM Pasquini, EF Soto, CP Setton-Avruj, *Dev. Neurosci.*, 2002, **24**, 214-221.
7. C Salis, C Davio, V Usach, N Urtasun, B Goitia, R MartinezVivot, *Neurochem. Int*, 2012, **61**, 798-806.
8. R Martinez Vivot, B Goitia, V Usach, PC Setton-Avruj, *Biofactors*, 2013, **39(4)**, 476-84.
9. D Ding, R Salvi, JA Roth, *Biometals*, 2014, **27**, 125–134.
- DR Richardson, V Neumannova, E Nagy, P Ponka, *Blood*, 1995, **86**, 3211-3219.
10. S Gruenheid, F Canonne-hergaux, S Gauthier, DJ Hackam, S Grinstein, P Gros, *J. Exp. Med.*, 1999, **189**, 831-841.
11. MA Su, CC Trenor, JC Fleming, DM Templeton, *Blood*, 1998, **92**, 2157-63.
12. M Tabuchi, T Yoshimori, K Yamaguchi, T Yoshida, F Kishi, *J. Biol.Chem.*, 2000, **275**, 22220-8.
13. MD Fleming, CC Trenor, D Foernzler, DR Beier, WF Dietrich, NC Andrews. *Nat. Genet.*, 1997, **16**, 383-386.
14. H Gunshin, B Mackenzie, UV Berger, Y Gunshin, MF Romero, WF Boron, S Nussberger, JL Gollan, MA Hediger, *Nature*, **388**, 482-488.
15. EA Farcich, EH Morgan. *Am J Hematol*, 1992, **39**, 9-14.
16. LM Garrick, KG Dolan, MA Romano, MD Garrick. Non-transferrin-bound iron uptake in Belgrade and normal rat erythroid cells. *J. Cell Physiol.*, 1999, **178**, 349-358.
17. R Ingrassia, A Lanzillotta, I Sarnico, M Benarese, F Blasi, L Borgese, *Plos One*, 2012, **7 (5)** e38019

- 1
 - 2
 - 3
 - 4
 - 5
 - 6
 - 7
 - 8
 - 9
 - 10
 - 11
 - 12
 - 13
 - 14
 - 15
 - 16
 - 17
 - 18
 - 19
 - 20
 - 21
 - 22
 - 23
 - 24
 - 25
 - 26
 - 27
 - 28
 - 29
 - 30
 - 31
 - 32
 - 33
 - 34
 - 35
 - 36
 - 37
 - 38
 - 39
 - 40
 - 41
 - 42
 - 43
 - 44
 - 45
 - 46
 - 47
 - 48
 - 49
 - 50
 - 51
 - 52
 - 53
 - 54
 - 55
 - 56
 - 57
 - 58
 - 59
 - 60
18. KR Jessen, R Mirsky. *Nat Rev Neurosci*, 2005, **6**, 671-682
19. R Mirsky, A Woodhoo, DB Parkinson, P Arthur-Farraj, A Bhaskaran, *J. Peripher. Nerv. Syst.*, 2008, **13**, 122-135.
20. AL Mescher, E Connell, C Hsu, C Patel, B Overton, *Dev. Growth Differ.*, 1997, **39**, 677-684.
21. WR Kiffmeyer, EV Tomusk, AL Mescher, *Dev. Biol.* 1991, **147**, 392-402.
22. G Raivich, MB Graeber, J Gehrman, GW Kreutzberg, *Eur. J. Neurosci.*, 1991, **3**, 919-927.
23. M DeUngria, R Rao, JD Wobken, M Luciana, CA Nelson, MK Georgieff, *Pediatr Res*, 2000, **48**, 169-176.
24. JL Beard, JR Connor, BC Jones, *Nutr. Rev.* 1993, **51**, 157-170.
25. JR Connor, SL Menzies, *Glia*, 1996, **17**, 83-93.
26. JL Beard, JR Connor, *Annu. Rev. Nutr.*, 2003, **23**, 41-58.
27. JL Beard, JA Wiesinger, JR Connor, *Dev. Neurosci*, 2003, **25**, 308-315.
28. CL Coe, GR Lubacha, L Bianco, JL Beard. *Dev. Psychobiol.*, 2009, **51**, 301-309.
29. CL Kwik-Urbe, D Gietzen, JB German, MS Golub, CL Keen, *J Nutr*, 2000, **130(11)**, 2821-30
30. MV Rosato-Siri, ME Badaracco, EH Ortiz, N Belforte, MG Clausi, EF Soto, R Bernabeu, JM Pasquini, *J. Neurosci. Res.*, 2010, **88(8)**, 1695-707
31. B Todorich., JM Pasquini, CI Garcia, PM Paez, JR Connor, *Glia*, 2009, **7**, 467-478.
32. ME Badaracco, EH Ortiz, EF Soto, J Connor, JM Pasquini, *J Neurosci. Res.* 2008, **86**, 2663-2673.
33. E Ortiz, JM Pasquini, K Thompson, B Felt, G Butkus, *J. Neurosci. Res.*, 2004, **77**, 681-689.
34. C Salis, CP Setton, EF Soto, JM Pasquini, *Exp. Neurology*, 2007, **207**, 85-94.
35. M Hadzhieva, E Kirches, C Mawrin, *Neuropathology and Applied Neurobiology*, 2014, **40 (3)**, 240–257.
35. P Urrutia, P Aguirre, A Esparza, V Tapia, NP Mena, M Arredondo, C González-Billault, MT Núñez, *J. Neurochem.*, 2013, **126**, 541–549.
37. J Wang, N Song, H Jiang, J Wang, J Xie, *Biochimica et Biophysica Acta*, 2013, **1832**, 618–625.
38. J Kim, RM Molina, TC Donaghey, PD Buckett., JD Brain, M Wessling-Resnick. *Am J Physiol Lung Cell Mol Physiol*, 2011, **300**, L659–L665.
39. JD Brain, E Heilig, TC Donaghey, MD Knutson, M Wessling-Resnick, RM Molina, *Am. J. Respir. Cell Mol. Biol.*, 2006, **34**, 330–337.
40. R Martini, S Fischer, R Lopez-Valez, S David, *Glia*, 2008, **56**, 1566–1577
41. AD Gaudet, PG Popovich, MS Ramer. *Journal of Neuroinflammation*, 2011, **8**,110-123
42. I Siglieti, M Bendszus , C Kleinschnitz , G Stoll . *J Neuroimmunol.*, 2006, **173(1-2)**, 166-73.
43. V Usach, B Goitia, L Lavallo, R Martinez Vivot, CP Setton-Avruj, *J. Neurosci. Res.*, 2011, **89(8)**, 1203-17.
44. L McKerracher, C Essagian, AJ Aguayo, *J Neurosci*, 1993, **13(6)**, 2617-26.
45. C Nicholls, H Li, JP Liu, *Clin. Exp. Pharmacol. Physiol.*, 2012, **39(8)**, 674-9.

- 1
2
3 46. V Zinchuk, O Zinchuk, T Okada, *Acta Histochem. Cytochem.*, 2007, **40**, 101-111.
4
5 47. K Livak, T Schmittgen, *Methods*, 2001, **25**, 405-408.
6
7 48. MC Leal, N Magnani, S Villordo, C Marino Buslje, P Evelson, EM Castaño, M Morelli, *J. Biol.*
8 *Chem.*, 2013, **288**, 12920-12931
9
10 49. GJ Copello, ME Villanueva, JA González, S López Egües, LE Diaz, *Journal of Applied Polymer*
11 *Science*, 2014, **131(21)**, 41005-41013
12
13 50. S Jenkitkasemwong, CY Wang, B Mackenzie, MD Knutson, *Biometals*, 2012, **25(4)**, 643-55.
14
15 51. ZK Attieh, Mukhopadhyay CK, Seshadri V, Tripoulas NA, Fox PL, *J. Biol. Chem.* 1999, **274(2)**,
16 1116-23.
17
18 52. B Todorich, X Zhang, B Slagle-Webb, WE Seaman, JR Connor, *J. Neurochem.*, 2008, **107(6)**,
19 1495-505
20
21
22
23
24
25
26
27
28
29
30
31
32
33
34
35
36
37
38
39
40
41
42
43
44
45
46
47
48
49
50
51
52
53
54
55
56
57
58
59
60

Figure legends

Figure 1. **DMT1 expression in SC at early stages of the demyelination-remyelination process.** Confocal microscopy of longitudinal sections of rat sciatic nerve 7 days post-injury. Column 1, Hoechst immunostaining; column 2, DMT1 immunoreactivity; column 3, immunoreactivity for S100 β ; column 4, merge of DMT1 and S100 β immunoreactivity. CTRL: control, CL: contralateral, P: proximal, C: crush, D: distal (60x), n=4.

Figure 2. **Persistence of DMT1 expression in SC at late stages of the demyelination-remyelination process.** Confocal microscopy of longitudinal sections of rat sciatic nerve 56 days post-injury. Column 1, Hoechst immunostaining; column 2, DMT1 immunoreactivity; column 3, immunoreactivity for S100 β ; column 4, merge of DMT1 and S100 β immunoreactivity. CTRL: control, CL: contralateral, P: proximal, C: crush, D: distal (60x), n=4.

Figure 3. **Increase in DMT1 protein levels after sciatic nerve crush.** A, Western blot slots (left panel) and their respective semi-quantification (right panel). B, evolution of DMT1 levels for the different areas as a percentage of a control sample. Values are expressed as the mean \pm SEM. The statistical analysis was performed by two-way ANOVA followed by DGC post-test, where letters (panel A) or asterisks (panel B) show groups significantly different with $p < 0.05$. CTRL: control, CL: contralateral, P: proximal, C: crush, D: distal, n=4.

Figure 4. **Increase in DMT1 mRNA after sciatic nerve crush.** qRT-PCR analysis of DMT1 mRNA evolution as fold-changes regarding a control sample. The inset shows the comparison of areas and a sham animal at each survival time. Values are expressed as the mean \pm SEM. The statistical analysis was performed by two-way ANOVA followed by

1
2
3 Tukey's post-test, where letters (panel A) or asterisks (panel B) show groups significantly
4 different with $p < 0.05$, $n=4$.

5
6
7 au: arbitrary units
8
9

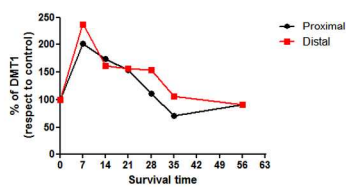
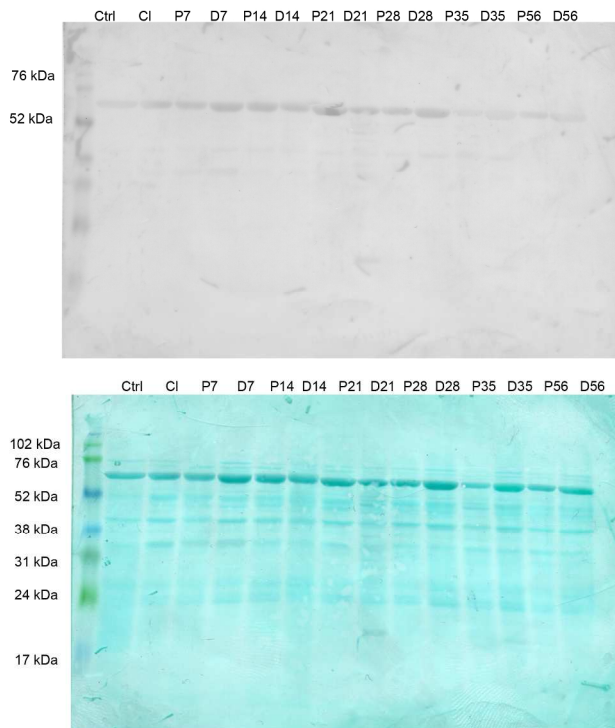
10
11 Figure 5. **Higher iron levels after sciatic nerve crush.** Atomic absorption
12 spectroscopy of iron contents in each area analyzed at different survival times regarding a
13 control sample. The inset shows the comparison of areas at each survival time. Values are
14 expressed as the mean \pm SEM. The statistical analysis was performed by two-way ANOVA
15 followed by DGC post-test, where letters (panel A) or asterisks (panel B) show groups
16 significantly different with $p < 0.05$, $n=4$.
17
18
19
20
21
22
23

24 Figure 6. **Relevance of DMT1 in remyelination.** The upper panel depicts the
25 demyelination-remyelination process separated in three stages: 1) ongoing demyelination
26 (1-14 dpi), 2) ongoing remyelination (15-35 dpi) and 3) remyelinated nerve (more than 35
27 dpi); the lower panel summarizes the evolution of DMT1 mRNA (green dotted line), DMT1
28 protein levels (green solid line) and iron content (purple line). MBP levels (yellow line) are
29 shown as a reference to the demyelination/remyelination process in our experimental
30 model.
31
32
33
34
35
36

37 dpi: days post-injury, Fe: iron content.
38
39
40

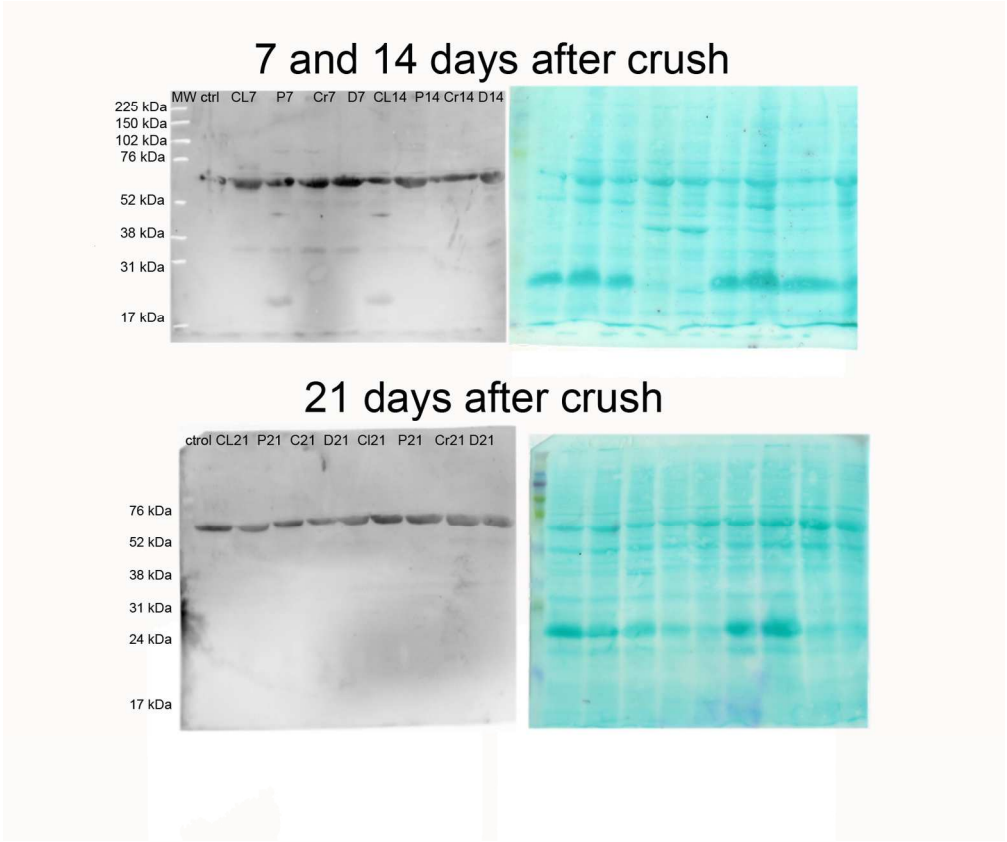
41 Table 1. **Correlation of DMT1 protein, transcript levels and iron content after**
42 **sciatic nerve crush.** Protein levels at each time point analyzed refer to their own
43 contralateral nerve. Asterisks indicate significantly different groups.
44
45
46
47
48
49
50
51
52
53
54
55
56
57
58
59
60

1
2
3
4
5
6
7
8
9
10
11
12
13
14
15
16
17
18
19
20
21
22
23
24
25
26
27
28
29
30
31
32
33
34
35
36
37
38
39
40
41
42
43
44
45
46
47
48
49
50
51
52
53
54
55
56
57
58
59
60



209x297mm (300 x 300 DPI)

1
2
3
4
5
6
7
8
9
10
11
12
13
14
15
16
17
18
19
20
21
22
23
24
25
26
27
28
29
30
31
32
33
34
35
36
37
38
39
40
41
42
43
44
45
46
47
48
49
50
51
52
53
54
55
56
57
58
59
60



150x126mm (300 x 300 DPI)

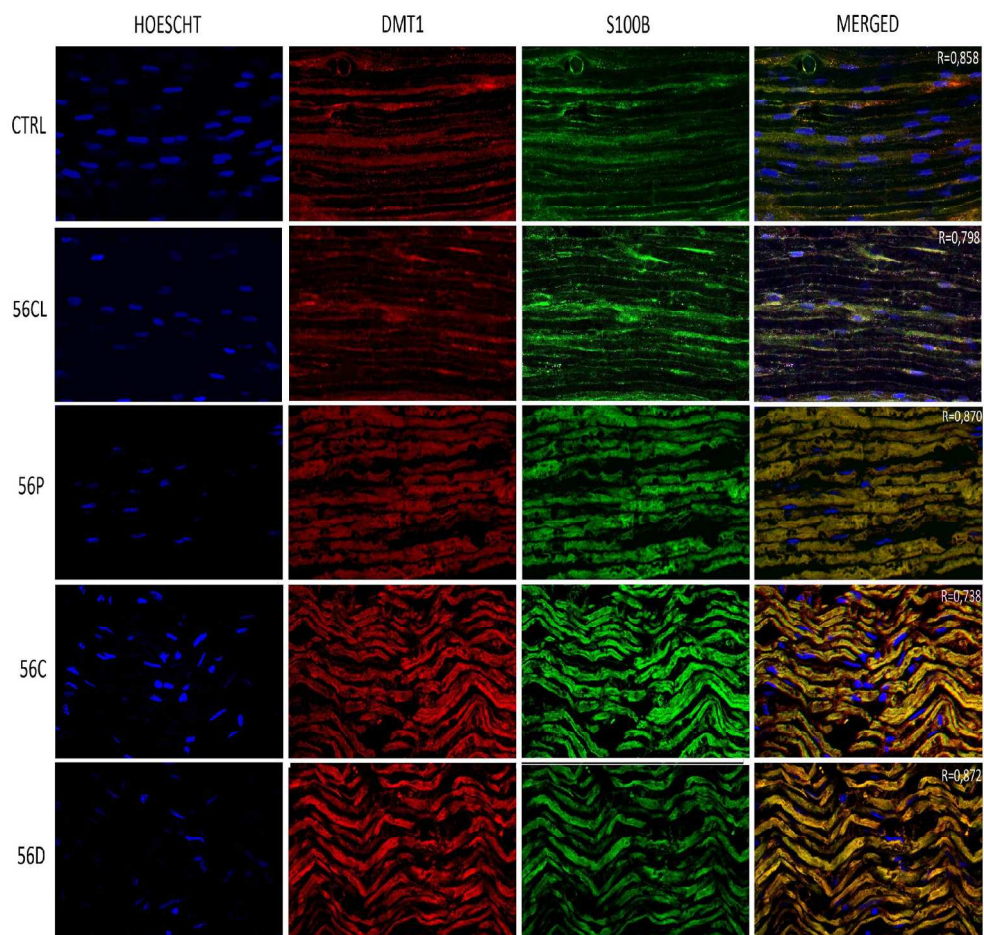


Figure 2. Persistence of DMT1 expression in SC at late stages of the demyelination-remyelination process. Confocal microscopy of longitudinal sections of rat sciatic nerve 56 days post-injury. Column 1, Hoechst immunostaining; column 2, DMT1 immunoreactivity; column 3, immunoreactivity for S100 β ; column 4, merge of DMT1 and S100 β immunoreactivity. CTRL: control, CL: contralateral, P: proximal, C: crush, D: distal (60x), n=4. 189x180mm (300 x 300 DPI)

1
2
3
4
5
6
7
8
9
10
11
12
13
14
15
16
17
18
19
20
21
22
23
24
25
26
27
28
29
30
31
32
33
34
35
36
37
38
39
40
41
42
43
44
45
46
47
48
49
50
51
52
53
54
55
56
57
58
59
60

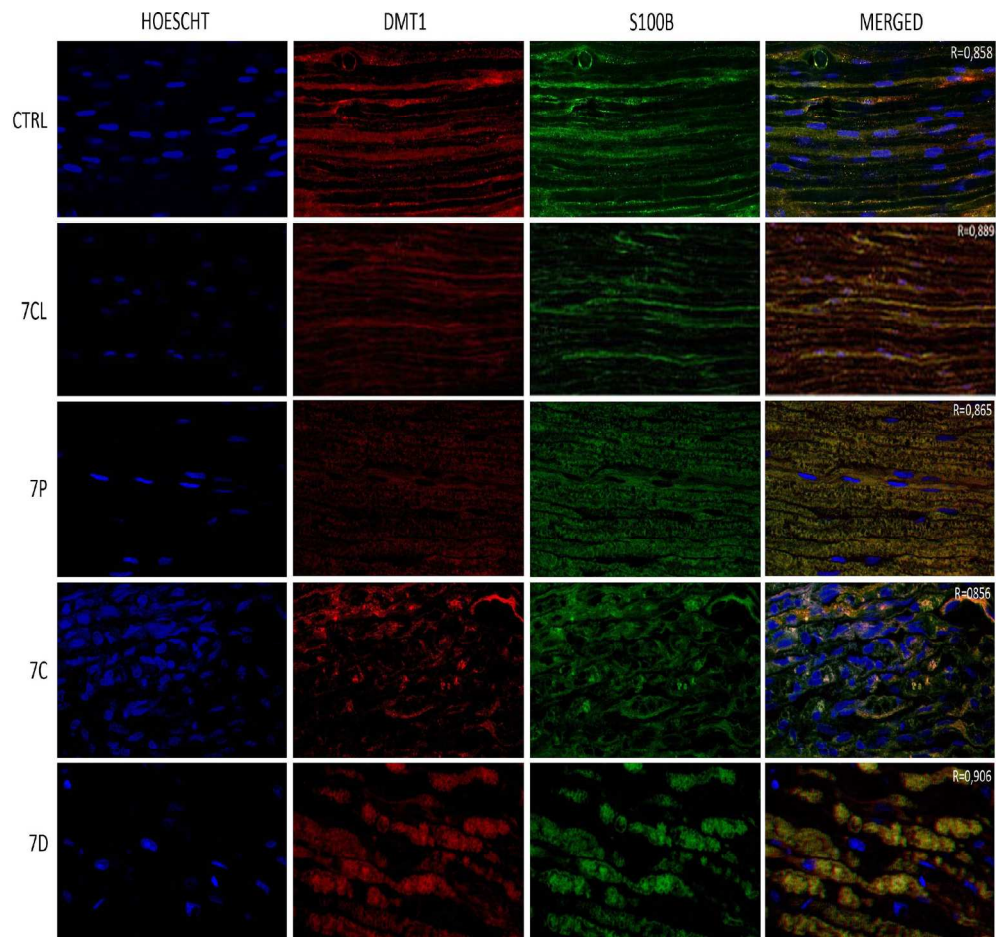


Figure 1. DMT1 expression in SC at early stages of the demyelination-remyelination process. Confocal microscopy of longitudinal sections of rat sciatic nerve 7 days post-injury. Column 1, Hoechst immunostaining; column 2, DMT1 immunoreactivity; column 3, immunoreactivity for S100 β ; column 4, merge of DMT1 and S100 β immunoreactivity. CTRL: control, CL: contralateral, P: proximal, C: crush, D: distal (60x), n=4. 189x180mm (300 x 300 DPI)

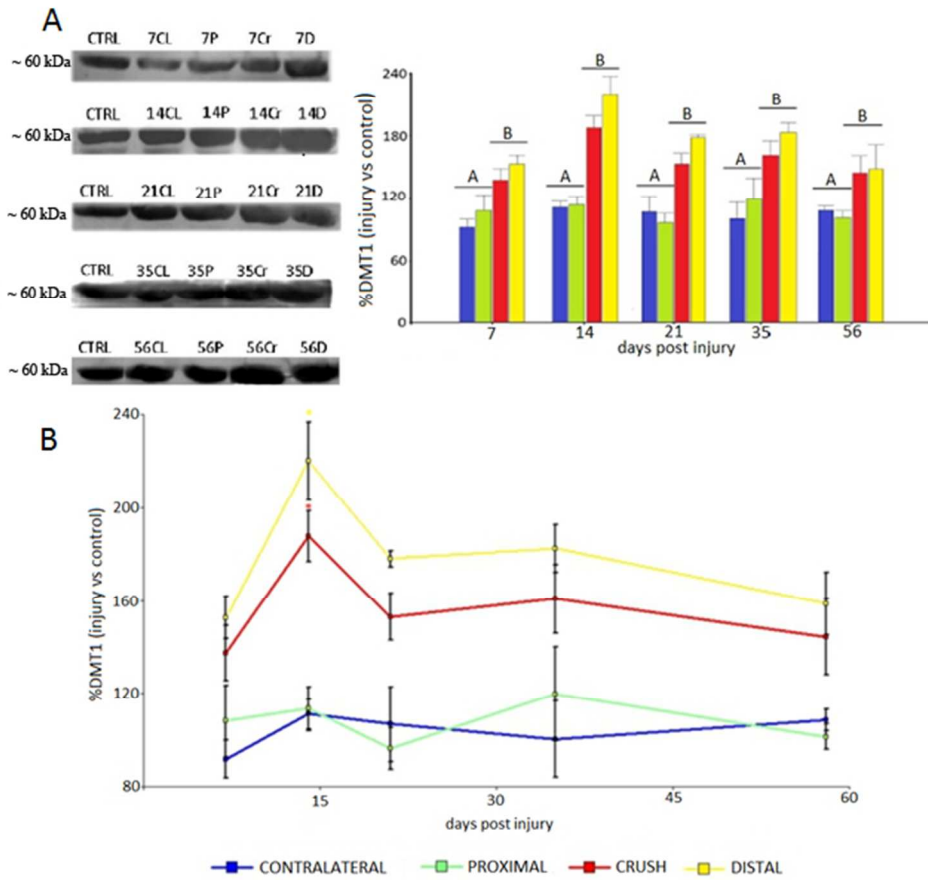


Figure 3. Increase in DMT1 protein levels after sciatic nerve crush. A, Western blot slots (left panel) and their respective semi-quantification (right panel). B, evolution of DMT1 levels for the different areas as a percentage of a control sample. Values are expressed as the mean \pm SEM. The statistical analysis was performed by two-way ANOVA followed by DGC post-test, where letters (panel A) or asterisks (panel B) show groups significantly different with $p < 0.05$. CTRL: control, CL: contralateral, P: proximal, C: crush, D: distal, $n=4$.

180x162mm (95 x 95 DPI)

1
2
3
4
5
6
7
8
9
10
11
12
13
14
15
16
17
18
19
20
21
22
23
24
25
26
27
28
29
30
31
32
33
34
35
36
37
38
39
40
41
42
43
44
45
46
47
48
49
50
51
52
53
54
55
56
57
58
59
60

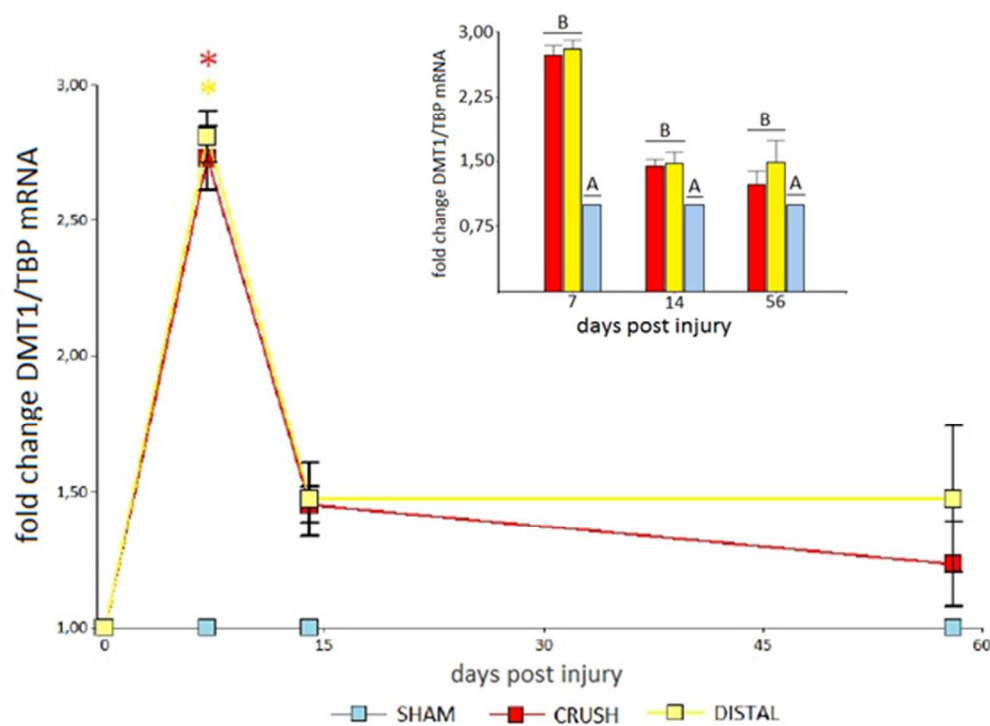


Figure 4. Increase in DMT1 mRNA after sciatic nerve crush. qRT-PCR analysis of DMT1 mRNA evolution as fold-changes regarding a control sample. The inset shows the comparison of areas and a sham animal at each survival time. Values are expressed as the mean \pm SEM. The statistical analysis was performed by two-way ANOVA followed by Tukey's post-test, where letters (panel A) or asterisks (panel B) show groups significantly different with $p < 0.05$, $n=4$.
au: arbitrary units

166x120mm (96 x 96 DPI)

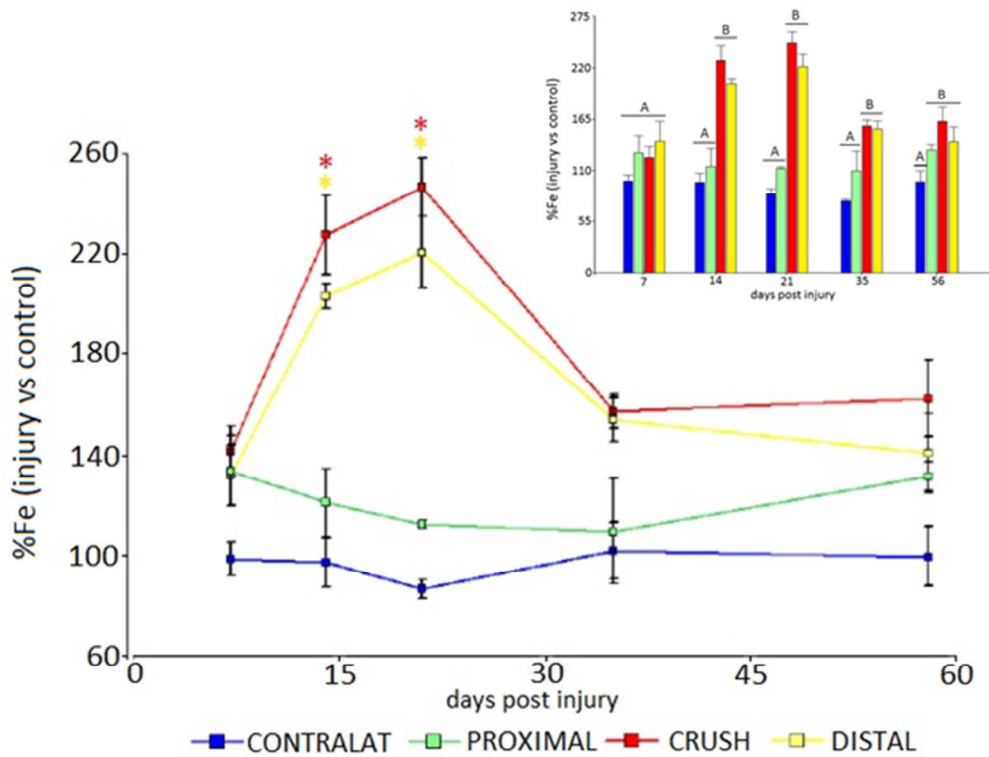


Figure 5. Higher iron levels after sciatic nerve crush. Atomic absorption spectroscopy of iron contents in each area analyzed at different survival times regarding a control sample. The inset shows the comparison of areas at each survival time. Values are expressed as the mean \pm SEM. The statistical analysis was performed by two-way ANOVA followed by DGC post-test, where letters (panel A) or asterisks (panel B) show groups significantly different with $p < 0.05$, $n=4$.
166x126mm (96 x 96 DPI)

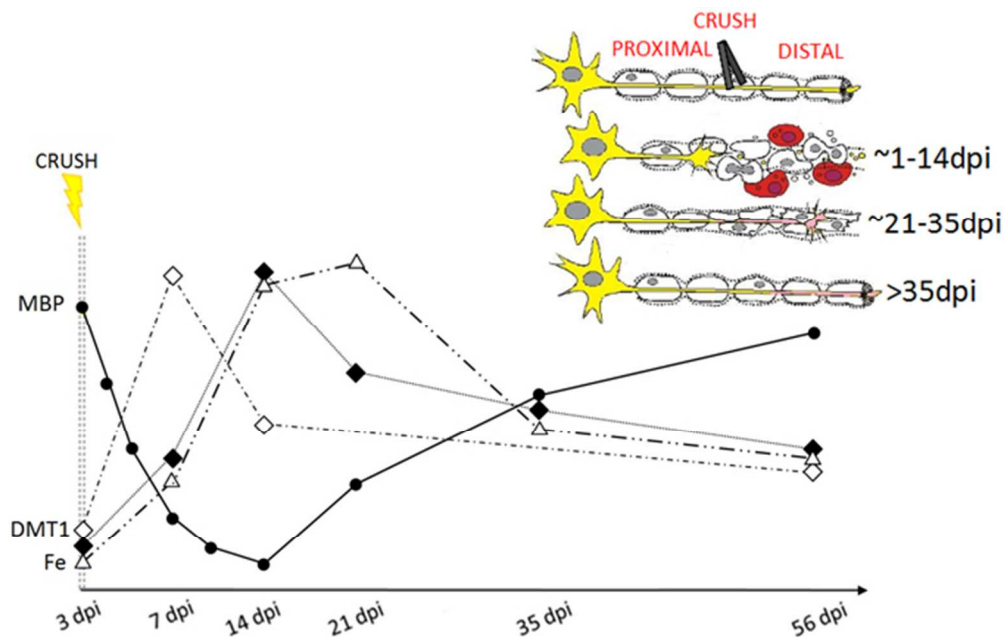


Figure 6. Relevance of DMT1 in remyelination. The upper panel depicts the demyelination-remyelination process separated in three stages: 1) ongoing demyelination (1-14 dpi), 2) ongoing remyelination (15-35 dpi) and 3) remyelinated nerve (more than 35 dpi); the lower panel summarizes the evolution of DMT1 mRNA (green dotted line), DMT1 protein levels (green solid line) and iron content (purple line). MBP levels (yellow line) are shown as a reference to the demyelination/remyelination process in our experimental model.

dpi: days post-injury, Fe: iron content.

179x114mm (96 x 96 DPI)

<u>Area</u>	<u>dpi</u>	<u>DMT1 protein level</u> (% increase)	<u>DMT1 mRNA</u> (fold change increase)	<u>iron content</u> (% increase)
<u>crush</u>	7	46*	1,73*	25
	14	77*	-	130*
	21	52*	-	161*
	35	60*	0,45*	80*
	56	36*	0,23*	64*
<u>distal</u>	7	61*	1,81*	42
	14	109*	-	106*
	21	74*	-	135*
	35	82*	0,47*	77*
	56	50*	0,47*	43*

Table 1. Correlation of DMT1 protein, transcript levels and iron content after sciatic nerve crush. Protein levels at each time point analyzed refer to their own contralateral nerve. Asterisks indicate significantly different groups.

208x96mm (96 x 96 DPI)

1
2
3
4
5
6
7
8
9
10
11
12
13
14
15
16
17
18
19
20
21
22
23
24
25
26
27
28
29
30
31
32
33
34
35
36
37
38
39
40
41
42
43
44
45
46
47
48
49
50
51
52
53
54
55
56
57
58
59
60